JOURNAL OF MATERIALS SCIENCE 27 (1992) 4515–4522

Solid phase change controlling the tensile and creep behaviour of gel-spun high-modulus polyethylene fibres

B. DESSAIN, O. MOULAERT, R. KEUNINGS
Unité de Mécanique Appliquée, Université Catholique de Louvain, Bâtiment Stévin, Place du Levant 2, 1348 Louvain la Neuve, Belgium

A. R. BUNSELL
Ecole Nationale Supérieure des Mines de Paris, Centre des Matériaux P.M. Fourt, B.P. 87, 91003 Evry Cédex, France

Tensile and creep tests have been conducted on monofilaments of gel-spun high-modulus polyethylene fibres. Fibre strength has been determined over a temperature range − 175–100 °C. The creep studies have revealed changes in behaviour which depend on the applied stress and the temperature. The results of these studies are explained by a change in crystallographic structure from orthorhombic to hexagonal which can take place under certain conditions of temperature and applied stress. It has therefore been possible to determine the applied stress necessary to obtain the change of phase as a function of temperature.

1. Introduction

It has long been realized that most polymers possess mechanical properties which are far from the maximum properties which are theoretically possible. This is due to the poor alignment of their molecular structure which results in intermolecular secondary bonds being stressed when a load is applied, rather than the primary bonds which control the integrity of the macromolecules. One approach to produce high-performance fibres has been to develop polymers based on increasingly rigid molecules containing a number of aromatic rings which give rise to liquid crystal technology and has resulted in the development of aramid fibres [1]. An alternative approach to the production of high-modulus organic fibres based on aligned simple linear molecules has developed since the 1970s [2–7]. This has given rise to the production of high-modulus gel-spun polyethylene fibres which possess mechanical properties similar to those of aramid fibres with an even lower specific gravity of 0.97. High-modulus polyethylene fibres of this type have been produced at laboratory level with Young's moduli up to 200 GPa, a tensile strength of 7 GPa and a 96% crystallinity [8, 9].

Commercially available gel-spun high-modulus polyethylene fibres are obtained by drawing from a solution with a 6% concentration of polyethylene. The control of the extraction and the recycling of the solvent are important features in the production of fibres by this method [10]. The technique allows the use of polyethylene of very high molecular weight of the order of 4×10^6 g mol^{-1}. This is to be contrasted to the molecular weight used in fibre production by melt spinning which is of the order of 250×10^3 g mol^{-1} and which possess inferior mechanical properties [10, 11].

It is known, however, that a major limitation to the use of polyethylene fibres is the temperature dependence of their mechanical properties. In the case of certain thermoplastics, including polyethylene, their temperature-dependent behaviour has been observed to be controlled by a phase change in the solid state [12–16]. Other polymers which undergo similar solid–solid phase changes are poly(*m*-methylene terephthalate) [17, 18] and poly(oxymethylene) [19]. This type of change in crystallographic structure can be brought about by the combined effects of temperature and applied stress.

It has been observed, for example, that poly(oxymethylene) undergoes a transformation from an orthorhombic to a triagonal structure when it is simultaneously heated to 70 °C and subjected to mechanical loading.

The present study examined the tensile and creep behaviour of single filaments of gel-spun polyethylene fibres. The experimental results suggest that their behaviour is controlled by a solid–solid phase change which is strongly dependent on the temperature and applied loading conditions.

2. Experimental procedure

The single filaments used in these experiments were gel-spun high-modulus polyethylene fibres (Dyneema SK60). Their nominal properties were a failure stress of 2.25 GPa, a Young's modulus of 68 GPa and a crystallinity of 80%.

0022–2461

TABLE I Tensile properties of Dyneema SK60 fibres as a function of temperature

T (°C)	N	σ_r(GPa)	S.D. σ_r(GPa)	E (GPa)	S.D. E (GPa)	ε_r (%)	S.D. ε_r(%)
− 175	4	3.76	0.08	114.1	13.8	4.92	0.37
− 160	11	3.59	0.43	111.7	12.6	4.54	0.34
− 125	12	3.56	0.33	111.1	9.6	4.76	0.33
− 100	11	3.4	0.24	106.9	10.1	4.77	0.27
− 60	11	3.23	0.39	92.5	5.9	4.97	0.42
− 30	11	3.03	0.3	87.6	14.3	4.8	0.41
0	14	2.86	0.51	72.5	4.7	5.23	0.71
24	12	2.25	0.33	67.6	9.8	4.89	0.58
40	18	2.00	0.32	59.6	9.0	4.35	0.65
70	16	1.39	0.16	39.8	4.1	7.23	1.03
100	13	0.60	0.07	29.3	6.8	15.87	1.62

The tensile and creep tests were conducted on a Universal Fibre Tester described in detail elsewhere [20]. This machine is capable of characterizing very fine filaments in tension, creep, relaxation and fatigue and has a load resolution in all these loading modes of 0.1 g. The distance between the jaws holding the fibre specimen is controlled by an electric motor and measured using a linear differential transducer with an accuracy of 1 μm. No particular preparation of the fibres was necessary before tensile and creep testing at room temperature and above; the fibres were simply gripped in the jaws between pieces of thin card to prevent damage. Tests below room temperature required the fibres being held by adhesive tape to a mounting card so that their rapid positioning in the machine was possible and an unduly important rise in temperature could be avoided. A resistance furnace was slid around the fibre for test at raised temperatures and in this case a specimen length of 150 mm was used. Tests were conducted at 40, 70 and 100 °C. Room-temperature tests were conducted using a number of different gauge lengths, at 23 °C and 50% relative humidity (r.h.). The speed of loading was 10 mm min^{-1}. The Universal Fibres Tester was fitted with a cold chamber, the temperature of which was varied using liquid nitrogen and which limited the fibres gauge length to 30 mm. Tests were conducted at 0, − 30, − 60, − 100, − 125, − 160 and − 175 °C.

Creep tests were conducted by requiring the machine to hold the load on the fibre steady at the chosen load. Initial loading was controlled so as to avoid any overshoot, so avoiding the problems associated with loading by dead weights and shock loading. The fibre tester is extremely stable and any variation in the load on the fibre greater than 0.1 g resulted in the electric motor switching on and adjusting the distance between the grips so as to return the fibre to the chosen load. Two conditions were considered, the first being with a fixed 70% of the average breaking load at each temperature being applied to the fibre at different temperatures, these being 25, 40, 55, 70, 85 and 100 °C. The second was with different applied loads corresponding to 50%, 60%, 70%, 80% and 85% of the average breaking load at each temperature and tests were conducted at 70 and 100 °C.

3. Results

The mean tensile strength, σ_r, modulus, E, and strain to failure, ε_r, are shown in Table I for different temperatures, together with the respective standard deviations. The number of fibres, N, tested at each temperature is also shown.

Typical load–elongation curves as a function of temperature are shown in Fig. 1 and the mean strengths as a function of temperature in Fig. 2. The evolution of the elastic moduli and strains to failure are shown, respectively, in Figs 3 and 4.

Creep tests were conducted at six different temperatures and at imposed loads representing 70% of the mean breaking load of the fibres at the temperature of that particular test. Table II shows the values used. The results obtained from this series of tests are shown in Table III which shows N, the number of tests under each condition, $\bar{\varepsilon}_r$, the average strain to failure, and $\bar{\varepsilon}$ the average of the strains to failure divided by the lifetimes and $\bar{\tau}$, the average lifetime. The parameters

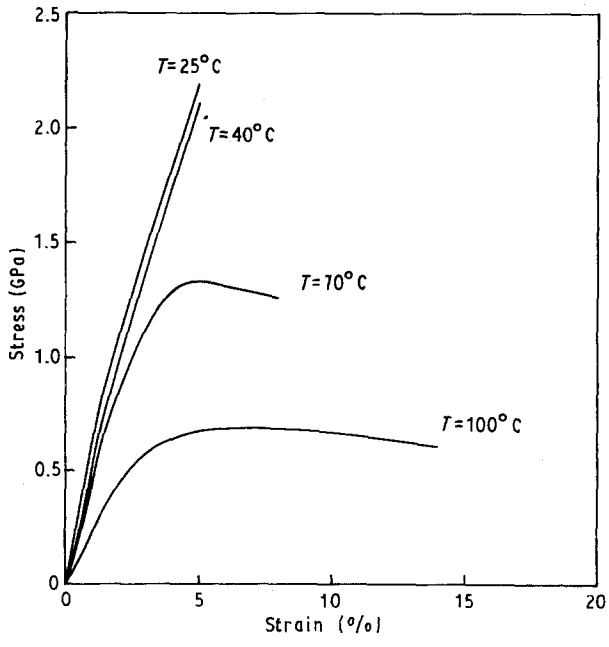

Figure 1 Load–elongation curves obtained at various temperatures.

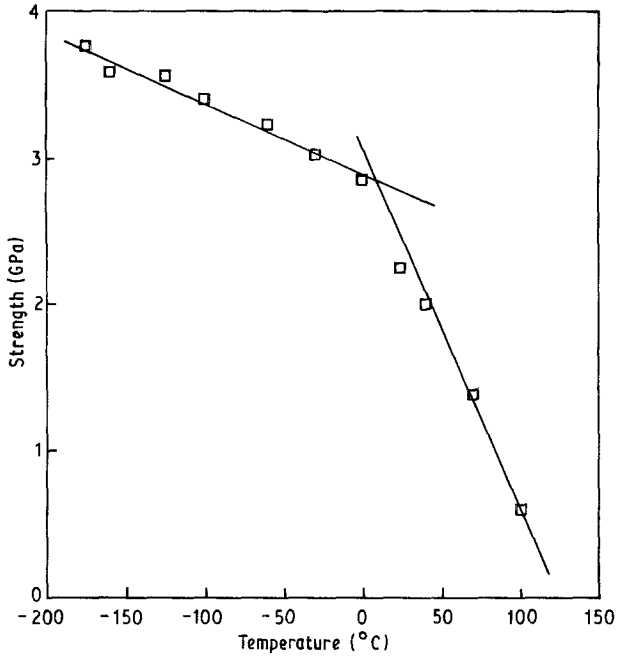

Figure 2 Evolution of mean strength as a function of temperature.

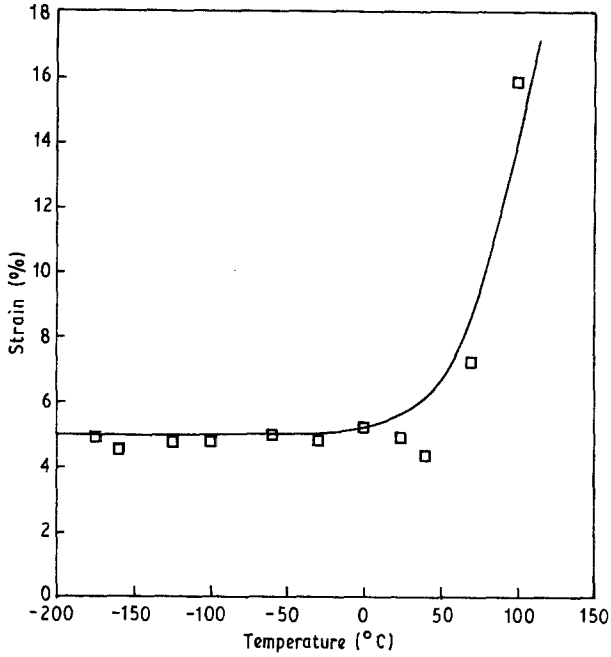

Figure 4 Strain to failure as a function of temperature.

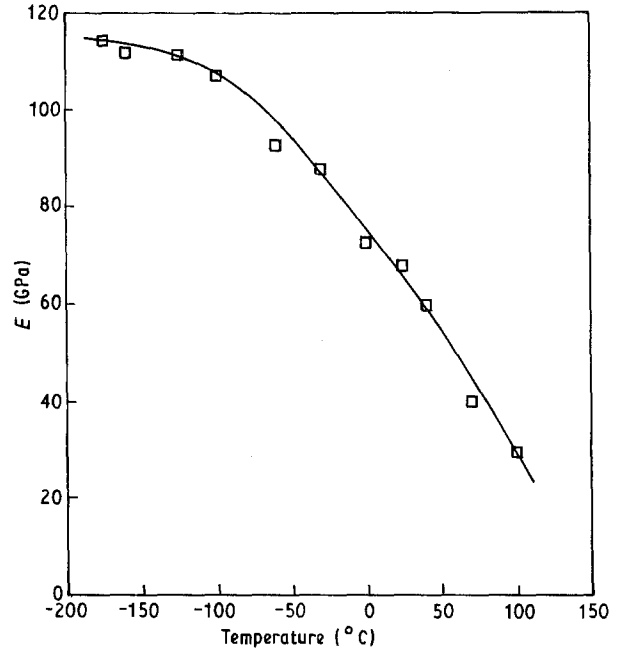

Figure 3 Evolution of elastic modulus as a function of temperature.

TABLE II Load and equivalent stress levels corresponding to 70% of the mean tensile strengths of the fibres used for creep tests at six different temperatures

	T (°C)					
	25	40	55	70	85	100
σ(GPa) = 70% σ_r	1.58	1.40	1.16	0.975	0.698	0.417
F(g) load	32.6	28.9	24.0	20.1	14.1	8.6

$\varepsilon_{1/2}$, $\tau_{1/2}$ and $\dot{\varepsilon}_{1/2}$ correspond to the median values of strains to failure, creep rates and lifetimes. Fig. 5 shows typical creep curves obtained under these conditions and Figs 6–8 reveal the variation of each parameter in Table III as a function of temperature.

Table IV shows the conditions employed for tests at different percentages of mean failure load, at temperatures of 70 and 100 °C. The results obtained at 100 °C are shown in Table V and at 70 °C in Table VI. Typical creep curves at 100 and 70 °C are shown, respectively, in Figs 9 and 10. The evolution of strain to failure, lifetime and strain rate at 100 and 70 °C are shown in Figs 11–16.

4. Discussion

It can be seen from Fig. 2 that the variations of fibre strength as a function of temperature show a distinct change of gradient at around 5 °C. Above this temperature, the fall in strength with temperature is considerably more marked than at lower temperatures.

TABLE III The result of creep tests at various temperatures (T) and 70% of the mean breaking stress at each temperature being applied

T (°C)	N	$\bar{\varepsilon}_R$ (%)	$\varepsilon_{1/2}$ (%)	$\bar{\tau}$ (s)	$\tau_{1/2}$ (s)	$\bar{\dot{\varepsilon}}$ (10^{-2} s^{-1})	$\dot{\varepsilon}_{1/2}$ (10^{-2} s^{-1})
25	10	7.15	6.4	7816	4170	0.16	0.14
40	10	8.05	7.6	3401	2267	0.34	0.21
55	10	10.10	9.6	2436	1916	0.54	0.45
70	10	13.28	12.9	1665	1303	0.94	0.78
85	10	17.00	16.6	1845	1264	1.14	0.95
100	8	20.16	19.3	1561	892	1.95	1.23

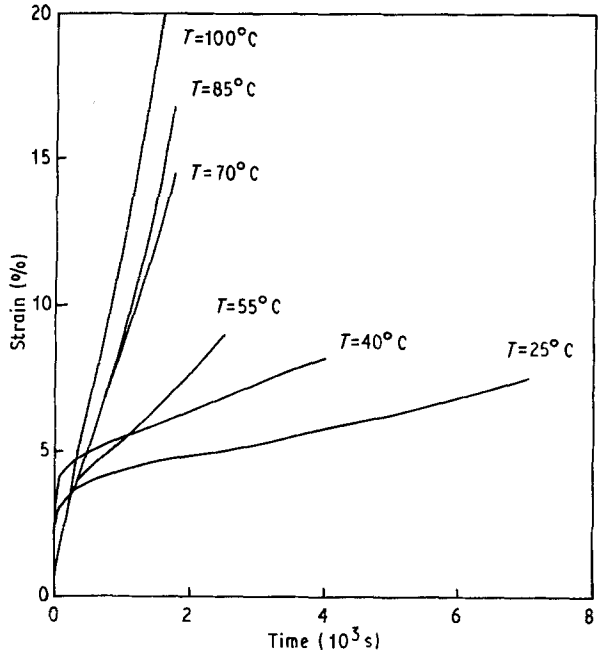

Figure 5 Creep curves obtained with 70% of breaking load applied at different temperatures.

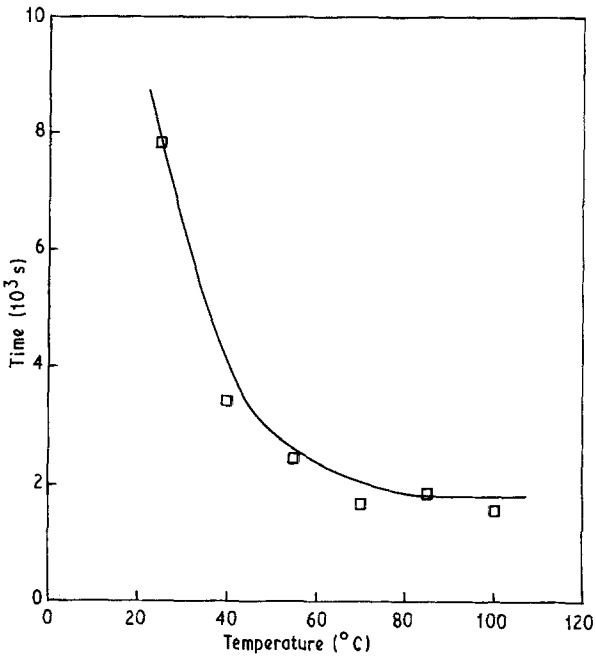

Figure 7 Creep lifetime as a function of temperature with 70% of breaking load applied.

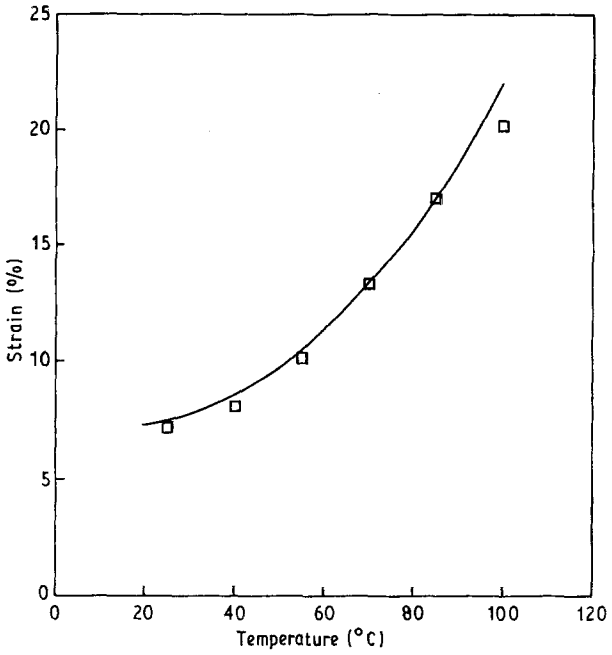

Figure 6 Strain to failure as a function of temperature with 70% of breaking load applied.

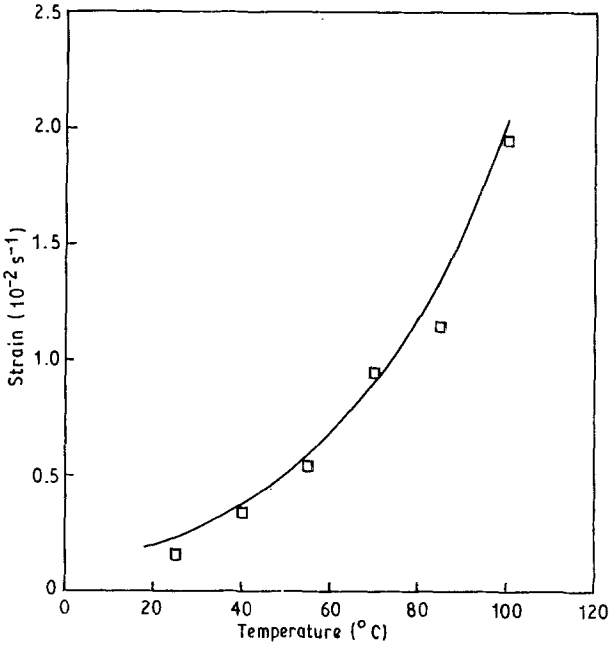

Figure 8 Creep rate as a function of temperature with 70% of breaking load applied.

TABLE IV Conditions for creep tests employed at 70 and 100 °C

T (°C)	σ_r (%)									
	50		60		70		80		85	
	σ (GPa)	F (g)	σ (GPa)	F (g)	σ (GPa)	F (g)	σ (GPa)	F (g)	σ (GPa)	F (g)
70	0.697	14.4	0.835	17.3	0.975	20.1	1.12	23.0	1.19	24.25
100	0.297	6.1	0.357	7.4	0.417	8.6	0.476	9.8	0.506	10.45

TABLE V Creep results obtained at various percentages of failure stress at 100 °C

σ_r(%)	N	$\bar{\varepsilon}_r$ (%)	$\varepsilon_{1/2}$ (%)	$\bar{\tau}$ (s)	$\tau_{1/2}$ (s)	$\bar{\dot{\varepsilon}}$ (10^{-2} s^{-1})	$\dot{\varepsilon}_{1/2}$ (10^{-2} s^{-1})
50	10	21.20	20.7	2957	2647	0.77	0.70
60	7	20.70	20.6	2217	1830	1.06	0.97
70	8	20.16	19.3	1561	802	1.95	1.23
80	5	18.12	17.6	624	518	3.10	2.80
85	6	17.53	17.4	556	540	3.30	3.50

TABLE VI Creep results obtained at various percentages of failure stress at 70 °C

σ_r(%)	N	$\bar{\varepsilon}_r$ (%)	$\varepsilon_{1/2}$ (%)	$\bar{\tau}$ (s)	$\tau_{1/2}$ (s)	$\bar{\dot{\varepsilon}}$ (10^{-2} s^{-1})	$\dot{\varepsilon}_{1/2}$ (10^{-2} s^{-1})
50	15	16.78	17.1	9194	6748	0.23	0.20
60	9	15.07	14.4	3142	2963	0.53	0.45
70	10	13.28	12.9	1665	1303	0.94	0.78
80	10	12.18	11.4	1293	782	1.22	1.02
85	12	8.50	8.5	306	209	3.50	3.20

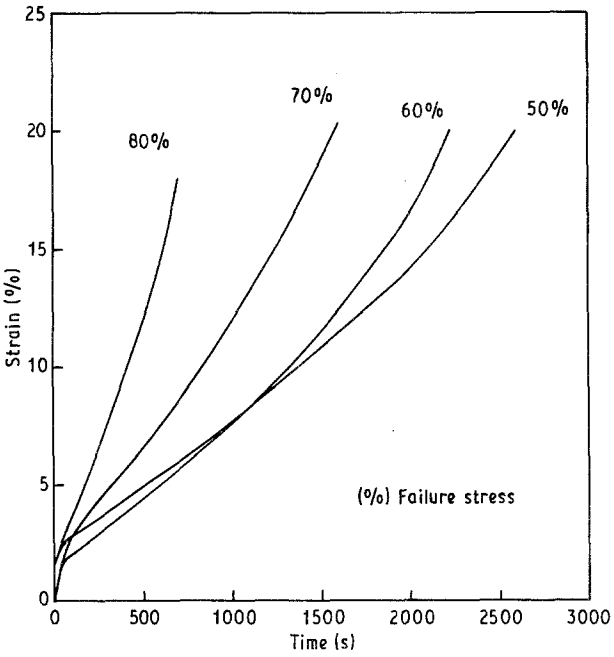

Figure 9 Creep curves obtained at 100 °C at different imposed loads.

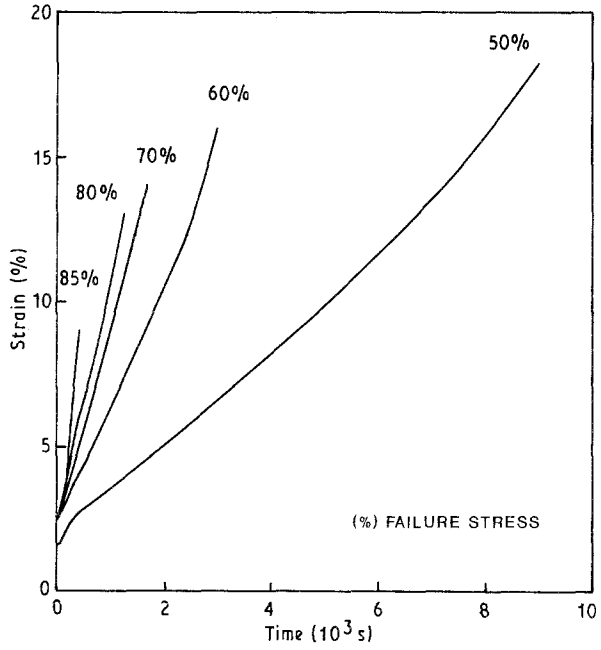

Figure 10 Creep curves obtained at 70 °C at different imposed loads.

This change in behaviour is most probably due to the solid phase change from orthorhombic to hexagonal as described by Dijkstra who examined laboratory spun fibres [11]. In the absence of an applied stress, this phase change occurs around 140 °C, just below the melting point at 146 °C. However, the phase change can be induced at lower temperatures if a stress is applied. The level of stress which has to be applied to achieve the phase change, (σ_ϕ), increases as the temperature is lowered until a critical point is reached below which the fibre fails under the applied stress before the phase change can occur. The results indicate that in the case of these high-modulus polyethylene fibres, this critical point is at 5 °C. Above this temperature the applied stress on the fibre results in a phase change and the structure becomes hexagonal. In this form the molecular chains are able to move by sliding more easily than in the orthorhombic phase and the material is strongly thermally dependent. Below 5 °C the orthorhombic form of the structure does not allow sliding and the temperature dependence of fibre tensile failure is controlled essentially by the C–C covalent bond.

The crystalline zones in these ultra-high-modulus polyethylene fibres are considered to be of the order of ten times longer than the intrafibrillar amorphous zones so that the crystalline phase plays a significant role in determining failure. However, it is likely that fracture involves the failure of taut tie-molecules in this intrafibrillar amorphous zone. In the orthorhombic phase it is unlikely that the tie molecules will be able to pull out of the crystalline blocks and their failure will involve the breaking of primary C–C bonds.

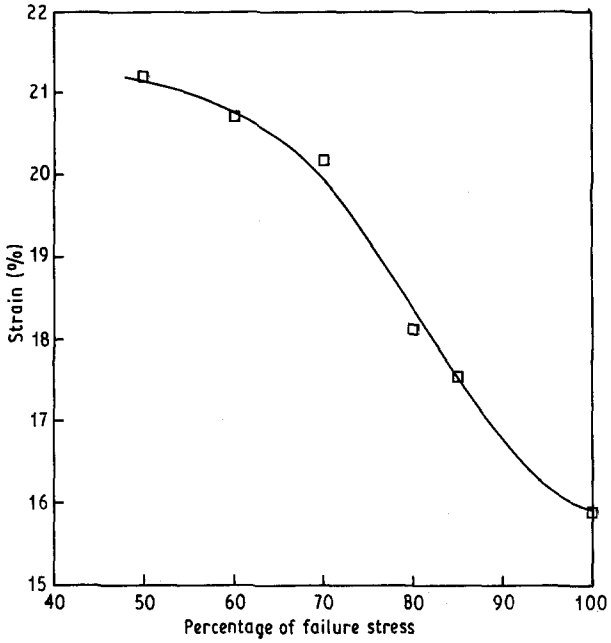

Figure 11 Strain to failure at 100 °C as a function of applied stress.

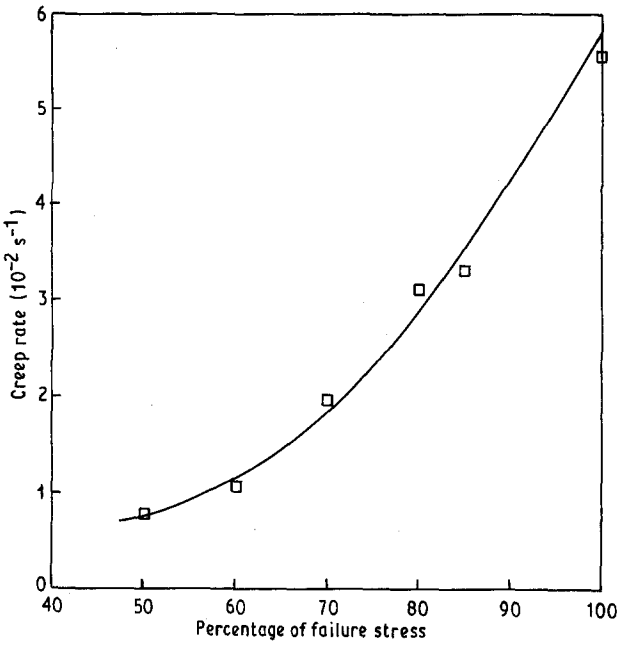

Figure 13 Creep rates as a function of applied stress at 100 °C.

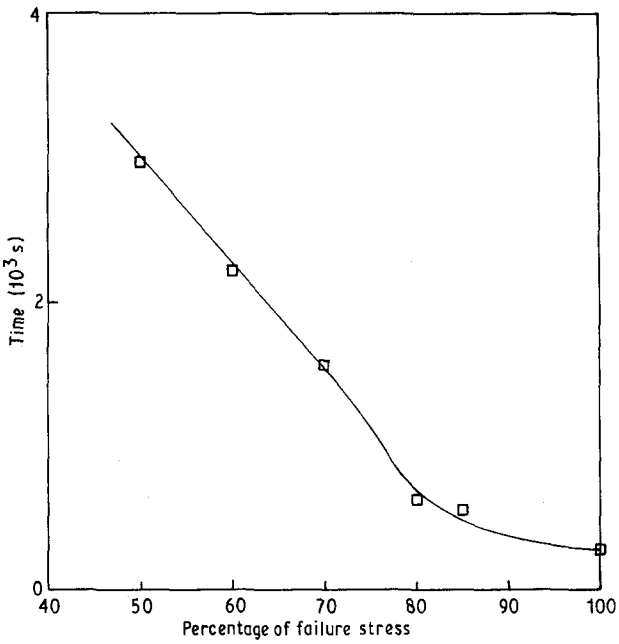

Figure 12 Creep lifetimes as a function of applied stress at 100 °C.

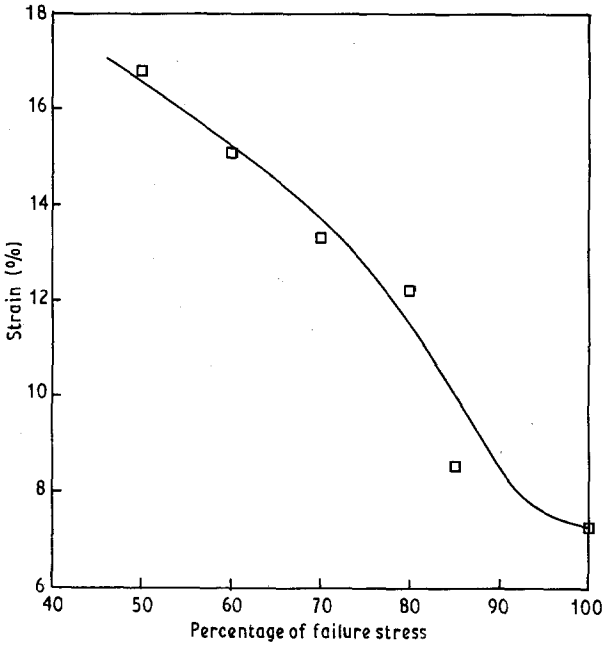

Figure 14 Strain to failure at 70 °C as a function of applied stress.

The hexagonal structure does, however, allow pull-out of the tie molecules and so modifies the fracture process, as slippage requires only failure of secondary bonds of the Van der Waals type. In many cases, however, the movement of the tie molecules must be restricted by entanglement and they may pass through several crystalline blocks. Ultimate failure in this case will depend both on the fracture of primary bonds of molecules which are trapped in the structure and on the failure of secondary bonds permitting slippage.

At 5 °C the stress which has to be applied to achieve the phase change equals that which causes failure, which is 2.74 GPa. Below this temperature the phase change becomes impossible. At 140 °C the stress necessary for the phase change falls to zero. At temperatures between these two extremes an applied stress can provoke the phase change. Figs 11 and 12 reveal that at 100 °C the curves of strain to failure and creep lifetime as a function of applied stress show an inflexion at around 75% of the tensile failure stress, or 0.447 GPa. At 70 °C the inflexion occurs at 1.47 GPa. This behaviour indicates that at temperatures below 5 °C the fibre breaks in the orthorhombic phase whilst above this temperature failure can either be in this phase for stresses lower than the critical phase transformation stress level or in the hexagonal phase at higher stress levels. It is now possible to plot the evolution of the phase transformation stress level, σ_ϕ, as a function of temperature as shown in Fig. 17.

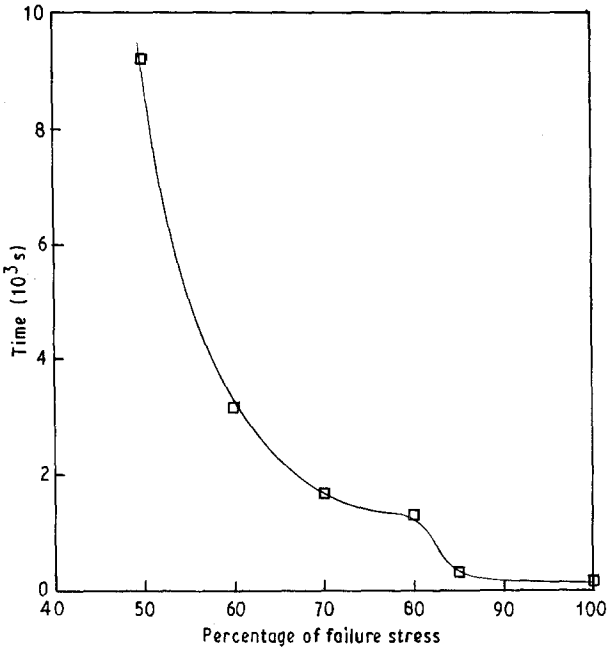

Figure 15 Creep lifetime as a function of applied stress at 70 °C.

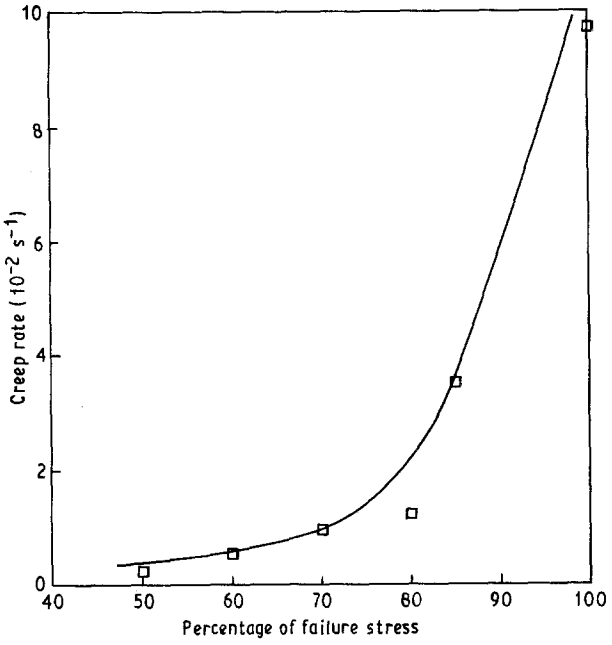

Figure 16 Creep rate as a function of applied stress at 70 °C.

5. Conclusions

Tensile and creep tests have been conducted on single gel-spun high-modulus polyethylene fibres. The tensile tests in the temperature range − 175–100 °C have revealed the strong temperature dependence of the failure stress of these fibres. This dependence shows a marked change at 5 °C, above which the effect of temperature becomes considerably more important. The creep tests have revealed behaviour which depended on the applied stress level and temperature. The points of inflexion which have been observed to occur in the curves of strain to failure as a function of applied load and creep lifetime as a function of applied stress at different temperatures indicate a crystallographic phase change as suggested by other authors

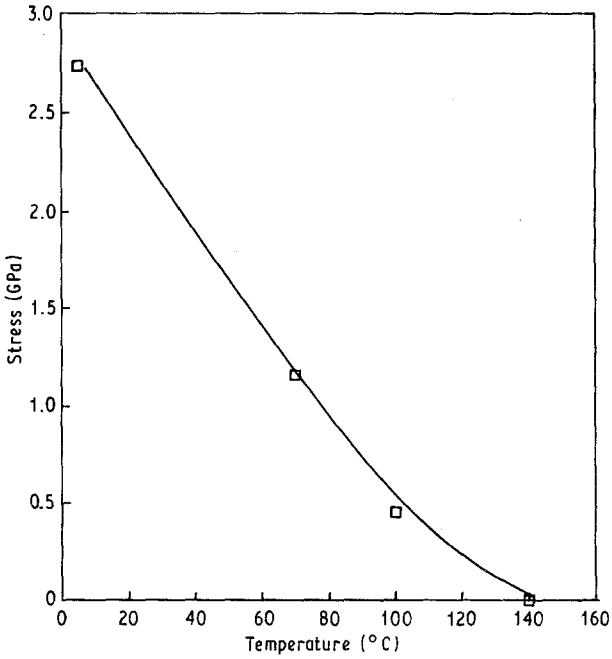

Figure 17 Evolution of phase transformation stress level as a function of temperature.

[11, 12]. This phase change from orthorhombic to hexagonal occurs in the absence of an applied load just below the melting point. An applied stress can provoke the phase change at lower temperatures, with the stress level necessary to produce the transformation increasing as the temperature decreases. At 5 °C, the stress necessary to produce the phase change equals that of the failure stress. Below 5 °C, no phase change can occur and the fibre structure remains orthorhombic. In this form the molecular structure has less possibility of movement and the temperature dependence of its mechanical properties is less marked than when the structure is transformed to the hexagonal phase. In this state molecular chain movement is facilitated and the temperature dependence of the fibre properties is considerably more marked.

Acknowledgements

This study has been conducted within the framework of the ERASMUS inter-university exchange programme between the Université Catholique de Louvain (Belgium) and l'Ecole Nationale Supérieure des Mines de Paris (France). The financial support from the French D.R.E.T., is acknowledged. The authors particularly thank Monsieur Y. Favry, ENSMP, for his considerable help during this study.

References

1. H. N. YANG, "Aramid Fibres, Fibre Reinforcements for Composite Materials", edited by A. R. Bunsell (Elsevier, Amsterdam, 1988) pp. 249–329.
2. A. ZWIJNENBURG and A. J. PENNINGS, *J. Polym. Sci. Polym. Phys.* **12** (1974) 635.
3. I. M. WARD, "The Stiffness and Creep Behaviour of Ultra High Modulus Polyethylene", in I.C.M. 3., Vol. 1, edited by K. J. Miller and R. F. Smith (Pergamon, 1979) pp. 353–67.
4. W. WU and W. B. BLACK, *Polym. Engng Sci.* **19** (1979) 1163.

5. J. H. SOUTHERN, N. WEEKS, R. S. PORTER and R. G. CRYSTAL, *Macromol. Chem.* **162** (1972) 19.
6. G. CAPACCIO and I. M. WARD, *Polymer* **15** (1974) 233.
7. *Idem, Polym. Engng Sci.* **15** (1975) 219.
8. C. SAWATARI and M. MATSUO, *Coll. Polym. Sci.* **263** (1985) 783.
9. A. V. SAVITSKII, I. A. GORSHKOVA, V. P. DEMICHEVA, I. L. FROLOVA and G. N. SHMIKK, *Polym. Sci. USSR* **26** (1984) 2007.
10. G. CALUNDAM, M. JAFFE, R. S. JONES and H. YAON, in "Fibre reinforcements for composite materials.", edited by A. R. Bunsell (Elsevier, Amsterdam, 1988) Ch. 5.
11. D. J. DIJKSTRA, PhD thesis, Rijks Universiteit, Groningen, (1988).
12. A. J. PENNINGS and A. ZWIJNENBURG, *J. Polym. Sci. Polym. Phys.* **17** (1978) 1011.
13. S. B. CLOUGH, *J. Macromol. Sci. Phys.* **B4** (1970) 199.
14. W. PECHHOLD, M. P. GROSSMAN and W. V. SODEN, *Coll. Polym. Sci.* **260** (1982) 248.
15. G. UNGAR, *Macromolecules* **19** (1986) 1317.
16. A. S. VAUGHAN, G. UNGON, D. C. BASSETT and A. KELLER, *Polymer* **26** (1985) 726.
17. I. M. WARD, M. A. WILDING and H. BRODY, *J. Polym. Sci. Polym. Phys.* **14** (1976) 263.
18. M. G. BRERETON, G. R. DAVIES, R. JAKEWAYS, T. SMITH and I. M. WARD, *Polymer* **19** (1978) 17.
19. M. KOBAYASHI, M. MORISHITA, M. SHIMOMURA and M. IGUCHI, *Macromolecules* **20** (1987) 2453.
20. A. R. BUNSELL, J. W. HEARLE and R. D. HUNTER, *J. Phys. E Sci. Instrum.* **4** (1971) 868.

Received 26 April
and accepted 13 May 1991